Research Article | Vol. 28, No. 9 / 27 April 2020 / Optics Express 12847
Optics EXPRESS

Role of polarization-mode coupling in the crosstalk between cores of weakly-coupled multi-core fibers

CRISTIAN ANTONELLI,[1,2,*] GABRIELE RICCARDI,[1] TETSUYA HAYASHI,[3] AND ANTONIO MECOZZI[1,2]

[1]Department of Physical and Chemical Sciences, University of L'Aquila, 67100 L'Aquila, Italy
[2]National Laboratory of Advanced Optical Fibers for Photonics (FIBERS), CNIT, L'Aquila, Italy
[3]Optical Communications Laboratory, Sumitomo Electric Industries, Ltd., 244-8588 Yokohama, Japan
[*]cristian.antonelli@univaq.it

Abstract: We develop a theory of crosstalk in weakly-coupled multi-core fibers that accounts for the effect of intra-core polarization-mode coupling. We show that random polarization-mode coupling plays a critical role, just like other polarization-independent effects such as fiber bending and twist, in explaining the observed incoherent crosstalk in weakly-coupled multi-core fibers.

1. Introduction

Space-division multiplexing (SDM) has been attracting significant attentions since the beginning of the past decade, and is considered to be an indispensable approacha to overcome the fundamental capacity limit of single-mode fiber-based transmission systems [1]. Multi-core fibers (MCFs) with nominally uncoupled cores are a promising candidate as the next-generation optical transmission medium for the implementation of SDM transmission over a single strand of optical fiber [2], and their core-to-core coupling/crosstalk characteristics have been intensively investigated [3–12]. The crosstalk is usually quantified in terms of a probabilistic parameter affected by various longitudinal perturbations of the MCF ideal structure. The longitudinal perturbations can be divided into low-spatial-frequency perturbations and high-spatial-frequency perturbations [8]. The low-spatial-frequency perturbations are caused by fiber macrobends and twists [3,5]. When the bend-induced core-to-core index perturbations are larger than the intrinsic core-to-core index mismatch (the so-called phase-matching region [8]), the mean crosstalk can be well predicted from the MCF structure and bending radius [5]. When the bend-induced core-to-core index perturbations are smaller than the intrinsic core-to-core index mismatch (the so-called non-phase-matching region [8]), more random and unpredictable high-spatial-frequency perturbations play an important role in the crosstalk. In order to take into account these random perturbations, Koshiba et al. [6] assumed an exponentially-decaying phase-term (i.e. the Euler exponential function of the phase) decorrelation between cores (resulting in a field-vector decorrelation function of the same type), and derived an analytical expression for the mean crosstalk in the non-phase-matching region [7] by assuming a proper correlation length of the core-to-core phase-term decorrelation for each MCF. The problem of this approach is that the correlation length can differ by orders of magnitude among MCFs [8,12,13], and cannot be predicted, it can only be extracted from crosstalk measurements of fabricated MCFs. We note, however, that the physical sources of the core-to-core phase decorrelation have not been fully elucidated yet. In early days, they were speculated to be the longitudinal structure fluctuations of the refractive index profiles of the cores [4,8], while more recently have been thought to be the random fiber twists under macrobends [9–12]. Besides these possible perturbation sources, strong microbends were experimentally confirmed to shorten the correlation length, or to increase the mean crosstalk in the non-phase-matching region [8]. Somehow surprisingly, these previous studies have disregarded

#391092 https://doi.org/10.1364/OE.391092
Journal © 2020 Received 21 Feb 2020; revised 3 Apr 2020; accepted 6 Apr 2020; published 15 Apr 2020

Optics EXPRESS

the effect of intra-core polarization-mode coupling spatial dynamics on the core-to-core phase decorrelation. While in fact, the strong mixing between orthogonal polarizations was advocated to explain the crosstalk chi-squared distribution [14], and to extend the discrete-changes model [5,15], its impact on the crosstalk magnitude has never been addressed directly. An exception to this general situation is constituted by [16], where intra-core polarization coupling is included in a more comprehensive model for the numerical study of the crosstalk temporal dynamics also in the nonlinear operation regime.

In this work, we study the effect of intra-core random polarization-mode coupling on the crosstalk of weakly-coupled MCFs. In doing so we take advantage of a 30-year-long heritage of theoretical and experimental studies on the birefringence statistics in single-mode fibers. We characterize the dependence of the average crosstalk on the birefringence strength and correlation, which are quantified through the beat length and correlation length [17] of the local birefringence vector [18], respectively. We show that intra-core random polarization-mode coupling alone, with typical values of beat length and correlation length reported in single-mode fiber characterizations, yields crosstalk levels that are consistent with those observed in state-of-the-art uncoupled MCFs. We also show that a crosstalk level reduction by multiple orders of magnitude can be achieved by either reducing the beat length or increasing the correlation length of the birefringence vector. The simple closed-form expressions for the average crosstalk coefficient resulting from the joint effect of random polarization-mode coupling that we derive may in principle serve as a handy tool to design low-crosstalk MCFs by controlling the perturbation statistics.

2. Crosstalk model

In this section we present a theory for the crosstalk between cores of a weakly-coupled multi-core fiber, as a result of linear mode coupling. In order to maintain the focus of the paper on the role of the intra-core random birefringence, other effects like polarization-dependent loss and Kerr-nonlinearity are neglected in the analysis. We denote the z-dependent Jones vectors of two continuous-wave polarized fields in two cores by $\vec{E}_n(z)$ and $\vec{E}_m(z)$. The evolution equation for $\vec{E}_n(z)$, in the framework of coupled-mode theory, can be expressed as follows [18,19]

$$\frac{\partial \vec{E}_n}{\partial z} = i\beta_{0,n}(z)\vec{E}_n + i\frac{\vec{\beta}_n(z)\cdot\vec{\sigma}}{2}\vec{E}_n + i\kappa_{nm}(z)\vec{E}_m, \tag{1}$$

where we omitted the terms accounting for the coupling with other cores for the sake of illustration simplicity. Here by $\beta_{0,n}(z)$ we denote the z-dependent propagation constant of the n-th core, which accounts for the fluctuations of the core effective index, as well as for the effect of fiber bending and twist. By $\vec{\beta}_n(z)$ we denote the birefringence vector in the same core, and by $\vec{\sigma}$ a vector whose elements are the three Pauli matrices, so that $\vec{\beta}_n\cdot\vec{\sigma} = \beta_{n,1}\sigma_1 + \beta_{n,2}\sigma_2 + \beta_{n,3}\sigma_3$ is the matrix describing local polarization-mode coupling [18]. Finally, the coefficient $\kappa_{nm}(z)$ quantifies the coupling between $\vec{E}_n$ and $\vec{E}_m$, as prescribed by coupled-mode theory [19], and its dependence on the longitudinal coordinate may reflect fluctuations in the core-to-core distance [20]. Note that the latter only couples identical polarization states in different cores. This is consistent with the fact that the local cores birefringence is smaller by orders of magnitude compared to the refractive index, and therefore the inter-core cross-polarization coupling coefficients for which it would be responsible are correspondingly small compared to the co-polarization coupling coefficient. By introducing the following definitions

$$\vec{e}_n(z) = e^{-i\theta_n(z)}\vec{E}_n(z) \tag{2}$$

$$\theta_n(z) = \int_0^z \beta_{0,n}(z')\mathrm{d}z', \tag{3}$$

Optics EXPRESS

(and equivalent definitions for $\vec{E}_m(z)$, whose evolution obeys Eq. (1) with n and m replaced one with the other), Eq. (1) becomes

$$\frac{\partial \vec{e}_n}{\partial z} = i\frac{\vec{\beta}_n(z)\cdot\vec{\sigma}}{2}\vec{e}_n + i\kappa_{nm}(z)e^{-i\Delta\theta_{nm}(z)}\vec{e}_m, \tag{4}$$

where $\Delta\theta_{nm}(z) = \theta_n(z) - \theta_m(z)$. Equation (4) generalizes Eq. (1) of [8] by accounting for the presence of random birefringence, whose effects are known to be crucial in single mode fiber propagation [18]. In the regime of weak coupling between cores, the second term is responsible for a perturbation to the zero-th order solution, which assuming that only core m is excited at the fiber input, is

$$\vec{e}_m(z) = \mathbf{U}_m(z,0)\vec{e}_m(0), \tag{5}$$

$$\vec{e}_n(z) = 0, \tag{6}$$

where the unitary matrix $\mathbf{U}_m(z,z_0)$ describes polarization evolution in core m from z_0 to z, and obeys the evolution equation [21]

$$\frac{\partial \mathbf{U}_m}{\partial z} = i\frac{\vec{\beta}_m(z)\cdot\vec{\sigma}}{2}\mathbf{U}_m. \tag{7}$$

The first-order solution for $\vec{e}_n(z)$ is therefore obtained by solving Eq. (4), where $\vec{e}_m(z)$ is replaced with its zero-th order solution. To this end, we first move to a rotating reference frame such that $\tilde{\vec{e}}_n(z) = \mathbf{U}_n^\dagger(z,0)\vec{e}_n(z)$, where Eq. (4) simplifies to

$$\frac{\partial \tilde{\vec{e}}_n}{\partial z} = i\kappa_{nm}(z)\mathbf{U}_n^\dagger(z,0)e^{-i\Delta\theta_{nm}(z)}\vec{e}_m, \tag{8}$$

which after integration with respect to z gives

$$\tilde{\vec{e}}_n(z) = i\int_0^z \mathrm{d}z'\kappa_{nm}(z')\mathbf{U}_n^\dagger(z',0)e^{-i\Delta\theta_{nm}(z')}\vec{e}_m(z'), \tag{9}$$

where by the dagger we denote Hermitian conjugation. Returning to the original reference frame and inserting Eq. (5) in the integral yields

$$\vec{e}_n(z) = i\int_0^z \mathrm{d}z'\kappa_{nm}(z')\mathbf{U}_n(z,z')e^{-i\Delta\theta_{nm}(z')}\mathbf{U}_m(z',0)\vec{e}_m(0), \tag{10}$$

where we used the property of the intra-core propagation matrix $\mathbf{U}(z,0)\mathbf{U}^\dagger(z',0) = \mathbf{U}(z,z')$ [18]. The physical interpretation of this expression is the following: the crosstalk originates from distributed coupling events, where the interfering field $\vec{e}_m(z)$ is polarization-rotated by the birefringence of the core in which is propagating until it couples at z' into the other core, whose birefringence keeps rotating its polarization to the fiber output. This process is accompanied by a polarization-independent phase accumulation in the two cores, which results in the phase difference $\Delta\theta_{nm}(z)$ appearing in the integral of (10). The average crosstalk power P_{nm} is evaluated as follows

$$\begin{aligned} P_{nm} &= \langle \vec{e}_n^\dagger(z)\vec{e}_n(z)\rangle \\ &= \int_0^z \mathrm{d}z' \int_0^z \mathrm{d}z''\kappa_{nm}^*(z')\kappa_{nm}(z'') \\ &\quad e^{i\Delta\beta_{nm}(z'-z'')}R_{ff}(z'-z'')\langle \vec{e}_m^\dagger(z')\mathbf{U}_n(z',z'')\vec{e}_m(z'')\rangle, \end{aligned} \tag{11}$$

where by angled brackets we denote ensemble averaging. In what follows we assume that $\kappa_{nm}(z) = \kappa_{nm}$ is independent of z. The effect of the fluctuations of the coupling coefficient is

Optics EXPRESS

studied in the Appendix, where we show that the assumption of constant κ_{nm} is well founded for moderate fluctuations of κ_{nm}, up to a few tens of percents. The term $e^{i\Delta\beta_{nm}(z'-z'')}R_{ff}(z'-z'') = \langle e^{-i[\Delta\theta_{nm}(z'')-\Delta\theta_{nm}(z')]}\rangle$ is discussed in detail in [8]. By $\Delta\beta_{nm}$ we denote the sum of the intrinsic term of the propagation constant mismatch between the two cores and its low-spatial-frequency fluctuations due to macro bending and twist, whereas the real-valued correlation function $R_{ff}(z'-z'')$ accounts for polarization-independent random structure fluctuations, to which in what follows we refer collectively as *scalar effects*. The low-spatial-frequency changes of $\Delta\beta_{nm}$ can be accounted for by further averaging the resulting crosstalk expression with respect to the statistics of macro-bending- and twist-induced phase fluctuations. However, in order to focus on the effects of polarization coupling, we refrain from performing this step in the present work, and therefore the average crosstalk expressions that we derive must be interpreted as quantifying the average crosstalk at a fixed fiber rotation angle. The average in the integral can be evaluated by noting that the two cores are characterized by independent birefringence processes, a fact that was observed in a recent experiment [22], and therefore the matrix $\mathbf{U}_n(z',z'')$ can be averaged separately first. Owing to the isotropy of the polarization mixing phenomenon, the average matrix must be proportional to the identity matrix, which in what follows we denote by $\mathbf{I}$. Moreover, assuming that each core's birefringence is a wide-sense stationary process, as is the case in single-mode fibers [17], the average matrix can only depend on $(z'-z'')$, which follows from noting that $\mathbf{U}(z'-z'',0)$ obeys the same equation as $\mathbf{U}(z',z'')$ where z' is replaced with $z'-z''$, namely

$$\langle \mathbf{U}_n(z',z'')\rangle = \langle \mathbf{U}_n(z'-z'',0)\rangle = R_n(z'-z'')\mathbf{I}. \tag{12}$$

The remaining average $\langle \vec{e}_m^{\dagger}(z')\vec{e}_m(z'')\rangle$ is obtained by using the stationarity argument along with Eq. (5), with the result $\langle \vec{e}_m^{\dagger}(z')\vec{e}_m(z'')\rangle = \vec{e}_m^{\dagger}(0)\langle \mathbf{U}_m(z'-z'',0)\rangle\vec{e}_m(0) = R_m(z'-z'')P_m$, where by $P_m = |\vec{e}_m(0)|^2$ we denote the power at the input of core m, and where by definition $R_m(z''-z') = R_m^*(z'-z'')$. Therefore the average crosstalk power expression, normalized to the input power, simplifies to the following form

$$\chi_{nm} = \frac{P_{nm}}{P_m} = 2\kappa_{nm}^2 \mathrm{Re}\left\{\int_0^z \mathrm{d}z' e^{i\Delta\beta_{nm}z'}(z-z')R_{ff}(z')R_n(z')R_m(z')\right\}. \tag{13}$$

In what follows the word *crosstalk* alone is used to refer to this quantity, unless otherwise specified. Note that this result, which was derived under the sole assumptions of isotropy and stationariety of the polarization-mode coupling process, is exact and general within the perturbation approach and applies to all types of MCFs, regardless of their design details (with the caveat that in the case of unequal cores the symbol κ_{nm} is meant to denote the average $(\kappa_{nm}+\kappa_{mn}^*)/2$, so as to ensure power conservation [6,23,24]). It shows that since $|R_{n,m}(z)|<1$, the effect of the polarization dynamics is most likely to reduce the average crosstalk [25,26]. In the regime of large propagation distance, where z exceeds by many times the width of $R_{ff}(z)$ and $R_{n,m}(z)$, the above simplifies to the familiar linear expression

$$\chi_{nm} = \alpha_{nm}z, \tag{14}$$

with

$$\alpha_{nm} = 2\kappa_{nm}^2 \mathrm{Re}\left\{\int_0^{\infty} \mathrm{d}z' e^{i\Delta\beta_{nm}z'}R_{ff}(z')R_n(z')R_m(z')\right\} \tag{15}$$

$$= \kappa_{nm}^2 \int_{-\infty}^{+\infty} \mathrm{d}z' e^{i\Delta\beta_{nm}z'}R_{ff}(z')R_n(z')R_m(z'), \tag{16}$$

which coincides with the result in Eq. (4) of [8], except for the presence of the product $R_n(z)R_m(z)$ describing polarization decorrelation in the two cores. The above is obtained by noting that the term $(z-z')$ can be replaced with z in the range of values of z' where the correlation functions product is significant, and then by extending the integral to the complementary range of values,

Optics EXPRESS

where the correlation functions product is vanishing and therefore its contribution to the integral is negligible. The coefficient α_{nm}, to which we refer as the crosstalk coupling coefficient, is the fraction of the power transferred per unit length from core m to core n, and vice versa. Equation (15) suggests an interesting classification of MCFs in terms of the dominant crosstalk-reduction mechanism. To see this, consider the case for which $\Delta\beta_{nm} = 0$, to which we refer as the case of *homogeneous MCFs*, and assume that the birefringence vector is characterized by the same statistics in all cores, in which case $R_n(z) = R_m(z) = R(z)$. Note that, since $\Delta\beta_{nm}$ is not just the propagation-constant mismatch, our definition of homogeneous MCFs implies not only that the cores have identical propagation constants, but also that the phase accumulated within the width of the function $|R_{ff}(z)R^2(z)|$ as a result of macro-bending and twist is much smaller than 2π. In this situation the average crosstalk is proportional to the integral of the product $R_{ff}(z)\mathrm{Re}\left\{R^2(z)\right\}$ and therefore homogeneous MCFs can be classified as follows: *polarization-coupled* fibers, for which $\mathrm{Re}\left\{R^2(z)\right\}$ is much narrower than $R_{ff}(z)$, and therefore random polarization coupling dominates inter-core coupling; *scalar-coupled* fibers for which $\mathrm{Re}\left\{R^2(z)\right\}$ is much wider than $R_{ff}(z)$, and therefore scalar effects set the coupling efficiency; *mixed-coupled* fibers where both effects are important. Needless to say that, in the first two classes, the non-dominant process can be safely neglected. It is therefore crucial to characterize the fiber birefringence for the analysis that follows. One universally accepted property of the birefringence is that its correlation function is the two-sided exponential [27,28]

$$\langle\vec{\beta}_n(z')\cdot\vec{\beta}_n(z'')\rangle = \left(\frac{2\pi}{L_{B,n}}\right)^2 e^{-\frac{|z'-z''|}{L_{C,n}}}, \tag{17}$$

where $L_{C,n}$ and $L_{B,n}$ are the correlation length and the beat length of the fiber birefringence vector, respectively. As we show in what follows, the knowledge of the correlation function of the birefringence vector is sufficient to characterize $R_n(z)$ in the regime of small correlation length, whereas in other regimes more details on the birefringence statistics are necessary. We note that Eq. (17) does not account for the effect of bending and twist on the accumulation of the birefringence vector and its statistics [29]. However, we expect that its inclusion will not affect the conclusions of the present work.

In the rest of the analysis, in order to derive simple analytic expressions for the average crosstalk coefficient, we assume that scalar effects are characterized by following correlation function

$$R_{ff}(z) = e^{-\frac{|z|}{\ell_c}}, \tag{18}$$

which is one of the forms (along with the Gaussian and triangular expressions) considered in [6]. Nonetheless, the conceptual implications of the analysis are valid also in the most general case, where a different expression for $R_{ff}(z)$ is considered [6,8].

2.1. Regime of small correlation length $L_{C,n} \ll L_{B,n}$

In this regime the two-sided exponential in the correlation function (17) can be replaced with its delta-function limit

$$\langle\vec{\beta}_n(z')\cdot\vec{\beta}_n(z'')\rangle = 2L_{C,n}\left(\frac{2\pi}{L_{B,n}}\right)^2\delta(z'-z''). \tag{19}$$

This is equivalent to describe fiber sections of length $\mathrm{d}z$ through uncorrelated zero-mean birefringence vectors $\mathrm{d}\vec{W}(z)$ with independent components of variance $2L_{C,n}(2\pi/L_{B,n})^2\mathrm{d}z/3$ [30,31]. The central limit theorem implies that in this case $\vec{\beta}_n(z)$ is a Gaussian vector with independent components, regardless of the statistics of $\mathrm{d}\vec{W}(z)$. Using the procedure reviewed in

Optics EXPRESS

the Appendix, in this regime one can find the following expression for $R_n(z)$,

$$R_n(z) = e^{-\frac{|z|}{\ell_n}}, \tag{20}$$

with

$$\ell_n = \frac{L_{B,n}^2}{\pi^2 L_{C,n}}, \tag{21}$$

and therefore the crosstalk at a generic propagation distance is given by

$$\chi_{nm} = 2\kappa_{nm}^2 \mathrm{Re}\left\{\frac{e^{-\left(\ell_{\mathrm{eq}}^{-1}+i\Delta\beta_{nm}\right)z} + \left(\ell_{\mathrm{eq}}^{-1} + i\Delta\beta_{nm}\right)z - 1}{\left(\ell_{\mathrm{eq}}^{-1} + i\Delta\beta_{nm}\right)^2}\right\}, \tag{22}$$

where we defined the equivalent length ℓ_{eq} as

$$\ell_{\mathrm{eq}}^{-1} = \ell_c^{-1} + \ell_n^{-1} + \ell_m^{-1}. \tag{23}$$

For $z \gg \ell_{\mathrm{eq}}$, the above yields the linear growth of Eq. (14) with

$$\alpha_{nm} = \frac{2\kappa_{nm}^2 \ell_{\mathrm{eq}}}{1 + \ell_{\mathrm{eq}}^2 \Delta\beta_{nm}^2}. \tag{24}$$

In the case of homogeneous cores with identical birefringence statistics ($\Delta\beta_{nm} = 0$, $L_{C,n} = L_{C,m} = L_C$ and $L_{B,n} = L_{B,m} = L_B$), for *polarization-coupled* MCFs ($\ell_c \gg \ell_n/2$) this yields the following simple result

$$\alpha_{nm} = \kappa_{nm}^2 \frac{L_B^2}{\pi^2 L_C}. \tag{25}$$

In the opposite regime of *scalar-coupled* MCFs ($\ell_c \ll \ell_n/2$) $\ell_{\mathrm{eq}} \simeq \ell_c$ and Eq. (24) yields the result of [7], $\alpha_{nm} = 2\kappa_{nm}^2 \ell_c$.

2.2. Regime of large correlation length $L_{C,n} \gg L_{B,n}$

The analysis of this regime relies on noting that for $|z - z'| \ll L_{C,n}$ one may assume the birefringence vector to be constant in the interval $[z', z]$ and approximate the n-th core transmission matrix $\mathbf{U}_n(z, z')$ as

$$\mathbf{U}_n(z, z') \simeq e^{i\frac{\vec{\beta}_n(z')\cdot\vec{\sigma}}{2}(z-z')}. \tag{26}$$

Averaging this expression requires the knowledge of the statistics of $\vec{\beta}_n(z')$, which cannot in general be deduced from its correlation function, and therefore further assumptions on the birefringence statistics are required. Two models consistent with the correlation function (17) are available in literature. One is known as the *random modulus model* (RMM) [27], and assumes that the third component of the birefringence vector, which describes circular birefringence, is zero, while its first and second components are described by two independent Ornstein-Uhlenbeck processes [30]. Within the RMM model, the steady state statistics of the birefringence is Gaussian and the average of Eq. (26) returns $\langle \mathbf{U}_n(z, z') \rangle = \exp\left[-\langle \vec{\beta}_n \cdot \vec{\beta}_n \rangle (z - z')^2/8\right] \mathbf{I}$, namely

$$R_n(z) = e^{-\frac{\pi^2}{2L_{B,n}^2} z^2}. \tag{27}$$

If the birefringence correlation length $L_{C,n}$ is much larger than the width of the Gaussian function at the right-hand side of (27), the expression obtained for $|z - z'| \ll L_{C,n}$ is a good approximation

Optics EXPRESS

for all values of z' in the integral of (15). In the case of homogeneous cores ($\Delta\beta_{nm} = 0$) and for $L_{B,n} = L_{B,m} = L_B$, this yields the following simple result

$$\alpha_{nm} = \kappa_{nm}\frac{L_B}{\sqrt{\pi}}\left[1 - \mathrm{erf}\left(\frac{L_B}{2\pi\ell_c}\right)\right] e^{\frac{L_B^2}{4\pi^2\ell_c^2}}. \tag{28}$$

which for *polarization-coupled* MCFs ($\ell_c \gg L_B$) simplifies to

$$\alpha_{nm} = \kappa_{nm}\frac{L_B}{\sqrt{\pi}}. \tag{29}$$

Note that (28) and (29) are independent of the birefringence correlation length. For *scalar-coupled* MCFs ($\ell_c \ll L_B$) Eq. (28) yields (using $\mathrm{erf}(x) \simeq 1 - \exp\left(-x^2\right)/\sqrt{\pi x^2}$) again the result of [7].

The other birefringence model consistent with the autocorrelation function (17) is known as the *fixed modulus model* (FMM) [32] and it assumes that the birefringence vector is of constant length, also lying in the equatorial plane of Stokes space, where its direction evolves following a random walk. The constant-modulus assumption of the FMM implies that at steady state the birefringence vector is uniformly distributed on a circle in the equatorial plane of Stokes space. This is unrealistic in weakly polarization-coupled cores, and its consequences in the limit $L_{C,n} \gg L_{B,n}$ make the results of this model unreliable. The pathological behavior of the FMM can be seen by expanding the exponential in Eq. (26) as [18]

$$\mathbf{U}_n(z, z') = \cos\left[\frac{|\vec{\beta}_n|(z - z')}{2}\right]\mathbf{I} + i\hat{\beta}_n(z')\cdot\vec{\sigma}\ \sin\left[\frac{|\vec{\beta}_n|(z - z')}{2}\right], \tag{30}$$

with $\hat{\beta}_n(z') = \vec{\beta}_n(z')/|\vec{\beta}_n|$, where $|\vec{\beta}_n|$ is the constant length of the birefringence vector, and by performing an ensemble averaging, which is responsible for the second term at the right-hand side of the equality to vanish. The result is the oscillatory function $R_n(z) = \cos(|\vec{\beta}_n|z/2)$ This produces a periodic power exchange between the two polarization eigenstates until the loss of coherence caused by the rotation of $\vec{\beta}_n$ takes over, which occurs only when $|z|$ becomes of the order of $L_{C,n}$. As a result, there are numerous oscillations of $R_n(z)$ within a correlation length. On the contrary, in the RMM the de-phasing is dominated by the fluctuations of the birefringence vector length, resulting into the Gaussian-shaped function of Eq. (27) — in fact Eq. (27) can also be obtained by further averaging the expression $R_n(z) = \cos(|\vec{\beta}_n|z/2)$ over the Rayleigh distribution of the birefringence vector length (a similar argument was used in [33] to explain the influence of the birefringence model on the prediction of the spin-induced reduction of polarization-mode dispersion in spun single-mode fibers). This difference explains the discrepancy between the RMM and the FMM in the regime of large correlation length, which is further discussed in section 3. We note that even in the absence of specific experimental evidences, it is unrealistic that the magnitude of the birefringence vector be rigorously uniform along the fiber, and this is the rationale for the use of the RMM in the analysis of this regime.

2.3. *Intermediate regime* $L_{C,n} \simeq L_{B,n}$

In the intermediate regime, where $L_{C,n}$ and $L_{B,n}$ are comparable, the FMM and the RMM yields similar results. Therefore, to study this regime we adopt the FMM, which allows to obtain closed-form analytical expressions for the average crosstalk. The derivation detailed in the Appendix yields the following expression for $R_n(z) = \langle \mathbf{U}_n(z, 0)\rangle$,

$$R_n(z) = Z_n^{(1)} e^{Y_n^{(1)}z} + Z_n^{(2)} e^{Y_n^{(2)}z}, \quad z \geq 0, \tag{31}$$

and $R_n(z) = R_n^*(-z)$ for $z<0$, where by the star we denote a complex conjugate, with

$$Z_n^{(1,2)} = \pm\frac{Y_n^{(1,2)} + L_{C,n}^{-1}}{Y_n^{(1)} - Y_n^{(2)}}, \tag{32}$$

Optics EXPRESS

$$Y_n^{(1,2)} = -\frac{1}{2L_{C,n}}\left(1 \pm \sqrt{1 - \frac{4\pi^2 L_{C,n}^2}{L_{B,n}^2}}\right). \tag{33}$$

Note that if $L_{B,n}>2\pi L_{C,n}$, then all coefficients in Eqs. (32) and (33) are real-valued, and the correlation function $R_n(z)$ consists of two negative-exponential functions. If, conversely, $L_{B,n}<2\pi L_{C,n}$, then the coefficients in Eqs. (32) and (33) are complex-conjugate in pairs and $R_n(z)$ assumes the form of a sinusoidal function enveloped by a negative-exponential function [34]. Finally, we note that in the regime of small correlation length ($L_{C,n} \ll L_{B,n}$) the coefficients in Eqs. (32) and (33) tend to $Y_n^{(1)} = -1/L_{C,n}$ and $Y_n^{(2)} = -\pi^2 L_{C,n}/L_{B,n} = -1/\ell_n$, $Z_n^{(1)} = 0$ and $Z_n^{(2)} = 1$, implying that the expression of $R_n(z)$ obtained within the FMM coincides with Eq. (20).

The product $R_n(z)R_m(z)$ can be expressed in the following form, for $z \geq 0$,

$$R_n(z)R_m(z) = \sum_{k=1}^{4} \eta_k e^{-\left(\ell_k^{-1} - i\Delta b_k\right)z}, \tag{34}$$

where the real-valued coefficients η_k, ℓ_k and Δb_k are defined through the equalities

$$\eta_{1,2} e^{-\left(\ell_{1,2}^{-1} + i\Delta b_{1,2}\right)z} = Z_n^{(1)} Z_m^{(1,2)} e^{\left(Y_n^{(1)} + Y_m^{(1,2)}\right)z}, \tag{35}$$

$$\eta_{3,4} e^{-\left(\ell_{3,4}^{-1} + i\Delta b_{3,4}\right)z} = Z_n^{(2)} Z_m^{(1,2)} e^{\left(Y_n^{(2)} + Y_m^{(1,2)}\right)z}, \tag{36}$$

and where Δb_k is possibly nonzero only if $Y_n^{(1,2)}$ and/or $Y_m^{(1,2)}$ are complex-valued (their dependence on n and m is omitted for notation simplicity). The average crosstalk expression is finally obtained in the following form

$$\chi_{nm} = 2\kappa_{nm}^2 \sum_{k=1}^{4} \eta_k \mathrm{Re}\left\{\frac{e^{-\left[\ell_{\mathrm{eq},k}^{-1} + i(\Delta\beta_{nm} + \Delta b_k)\right]z} + \left[\ell_{\mathrm{eq},k}^{-1} + i(\Delta\beta_{nm} + \Delta b_k)\right]z - 1}{\left[\ell_{\mathrm{eq},k}^{-1} + i(\Delta\beta_{nm} + \Delta b_k)\right]^2}\right\}, \tag{37}$$

$$\alpha_{nm} = 2\kappa_{nm}^2 \sum_{k=1}^{4} \eta_k \frac{\ell_{\mathrm{eq},k}}{1 + \ell_{\mathrm{eq},k}^2(\Delta\beta_{nm} + \Delta b_k)^2}, \tag{38}$$

where we defined $\ell_{\mathrm{eq},k}^{-1} = \ell_c^{-1} + \ell_k^{-1}$. In the absence of polarization coupling, in which case $\ell_k \to \infty$ and $\Delta b_k = 0$, one can readily check that the above is consistent with the result of [7].

3. Results

In Fig. 1 we illustrate the dependence of the average crosstalk on the beat length and correlation length of the fiber birefringence. Since in this work we are mainly interested on the effect of polarization coupling on crosstalk, we focus on the case of *polarization-coupled* MCFs, where polarization effects are dominant. We consider a homogeneous MCF ($\Delta\beta_{nm} = 0$), with cores occupying the vertexes of a square, and with identical birefringence statistics in all cores ($L_{C,n} = L_{C,m} = L_C$ and $L_{B,n} = L_{B,m} = L_B$) and plot the crosstalk coefficient α_{nm} versus the birefringence correlation length L_C for three values of the beat length L_B which are consistent with values observed in single-mode fibers [35]. In this example we set the coupling coefficient between nearest neighbor cores to $\kappa_{nm} = 4.5 \times 10^{-5}$ m^{-1} and neglected the coupling between the others. The thick lines are the plot of the expressions in Eqs. (25) and (29), obtained in the two regimes of small and large correlation length, respectively, while the thin dashed line is the plot of the FMM result Eq. (38). As anticipated in section 2.2, the FMM curve deviates from the RMM result for large values of the birefringence correlation length.

Optics EXPRESS

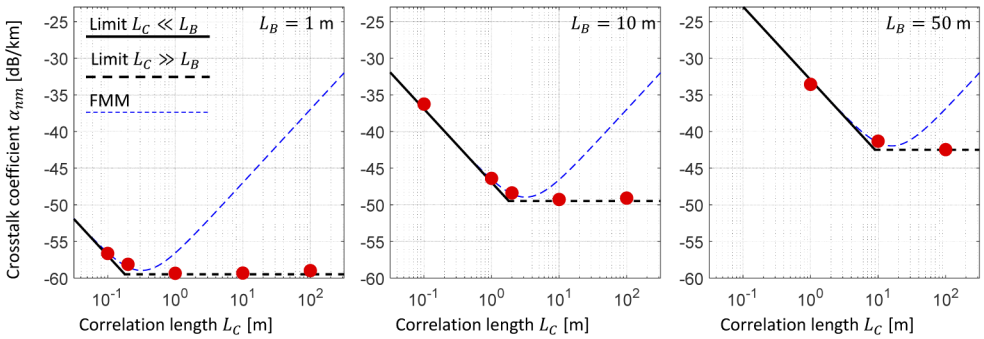

Fig. 1. Crosstalk coefficient versus the birefringence correlation length for the displayed values of the birefringence beat length. The plots refer to the case of a homogeneous MCF with identical birefringence statistics in the various cores. The thick solid and dashed lines are the plot of Eqs. (25) and (29), respectively, while the thin dashed lines refer the FMM. The dots show the results of Monte-Carlo simulations.

Consistent with the intuition, the figure shows that by either increasing the birefringence strength or its correlation length the average crosstalk reduces. However the latter effect saturates at the point where the correlation length is sufficiently large that the birefringence vector is approximately uniform (yet still random) over a distance of the order of the beat length. Most remarkably, the figure shows that low crosstalk levels can always be attained for specific combinations of L_C and L_B values. Obviously this also implies that by simultaneously accounting for polarization-independent random structure fluctuations and random polarization coupling, a given crosstalk level can be attained for a number of combinations of L_C and L_B and ℓ_c. The analysis illustrated in Fig. 1 was validated by comparison with Monte Carlo simulations with 1,000 repetitions, whose results are plotted by dots. In the numerical simulations we made use of the RMM for generating the fiber birefringence. The details of the numerical simulations are described in the Appendix.

It is also interesting to note that very small values of the crosstalk coefficient can be obtained with low values of the birefringence beat lengths (see the first panel of Fig. 1, which refers to $L_B = 1$ m), even in the absence of other polarization-independent coupling mechanisms. This suggests that in principle introducing some controlled random birefringence in the fiber manufacturing process (ideally by making the cores slightly elliptical and by randomly changing the ellipse axes) may result into ultra-low crosstalk levels.

It is important to note that the consideration of polarization-mode coupling does not affect the crosstalk statistics. Indeed, inspection of Eq. (10) suggests that if propagation distance is several times larger (on the order of tens to hundreds) than the lengths over which the polarization and scalar effects decorrelate, then the accumulated interfering field results from many independent random contributions, and hence by the central limit becomes a Gaussian vector with 2 complex components. Therefore the crosstalk can be approximated with a chi-squared distributed variable with 4 degrees of freedom (two quadratures and two orthogonal polarizations) [14,36], a conclusion which is also in agreement with recent experimental findings [37]. This property is not affected by the presence of multiple interfering cores, as the contributions of the various cores are practically independent of each other. In this case the average crosstalk results from the contributions of the individual cores. The crosstalk distribution is investigated by means of Monte Carlo simulations in Fig. 2 for the same homogeneous four-core fiber of Fig. 1 with $L_C = 10$ m. In the panels on the left we plot the average crosstalk in the fourth core of the fiber section in the inset when the first, second, and third cores are excited at the fiber input with a randomly polarized field of unit power. The dotted lines are the result of Monte Carlo simulations

Optics EXPRESS

with 100,000 repetitions, while by solid lines we plot the FFM-based theoretical result Eq. (38). The panels in the middle show the corresponding standard deviations, whereas in the panels on the right we plot the crosstalk probability density function at $z = 1$ km (the solid curve is the plot of a chi-squared probability density function with the theoretical average). Top and bottom panels refer to the two cases in which the birefringence beat length L_B is 0.8 times smaller and 1.2 times greater than $2\pi L_C$, respectively, two values that fall in the regime of intermediate correlation length that is well described by the FMM and cover the two classes of solutions in Eqs. (32) and (33). The good agreement between theory and simulations is self-evident.

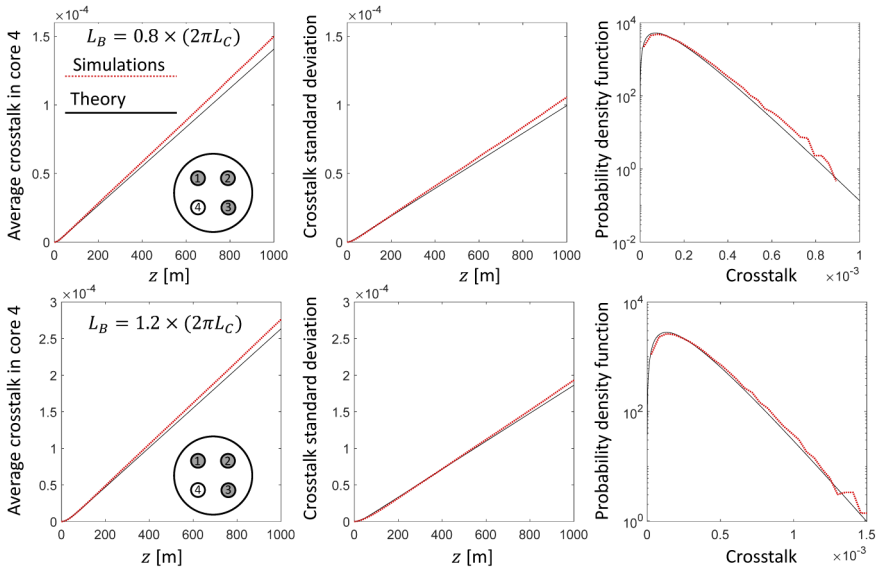

Fig. 2. The left panels show the average crosstalk affecting core 4 when cores 1, 2, and 3 are excited with independent randomly polarized fields of identical intensity. The optical power in core 4 is normalized to the power at the input of the other cores. The middle panels show the corresponding crosstalk standard deviation, and the right panels the crosstalk probability density function at $z = 1$ km. Top panels and bottom panels refer to the two cases $L_B = 0.8 \times (2\pi L_C)$ and $L_B = 1.2 \times (2\pi L_C)$, respectively, which both belong to the regime of small correlation length of Fig. 1.

4. Conclusions

Previous studies of crosstalk in weakly-coupled multi-core fibers addressed the role of random polarization-mode coupling somehow elusively. Aim of this work is to clarify the relevance of intra-core polarization dynamics in the accumulation of inter-core coupling along the fiber. By hinging on 30 years of theoretical and experimental studies on the statistics of random birefringence in single-mode fibers, we developed a crosstalk theory that accounts for intra-core polarization coupling spatial dynamics. We characterized the dependence of the average crosstalk power on the main parameters of the birefringence statistics, which are the correlation length and the beat length of the birefringence vector used in polarization studies to describe the local fiber birefringence, and provide simple closed-form expressions for it. We showed that for values of beat length and correlation length that are typically measured in single-mode fibers, polarization coupling alone may yield crosstalk levels that are consistent with experimental observations. We also showed that the crosstalk can be reduced by either reducing the birefringence beat length

Optics EXPRESS

or by increasing the correlation length. In principles this paves the ground for the design of low-crosstalk multi-core fibers based on introducing perturbation with controlled statistics.

Appendix

Derivation of $\langle \mathbf{U}_n(z,0)\rangle$ *in the regime of small correlation length*

In this regime the birefringence vector of a fiber section of length $\mathrm{d}z$ can be described by means of the vector $\mathrm{d}\vec{\beta}_n(z) = \sqrt{D_n}\mathrm{d}\vec{W}_n(z)$, where $D_n = 2L_{C,n}(2\pi/L_{B,n})^2\mathrm{d}z$ and where the three components of $\mathrm{d}\vec{W}_n(z)$ are independent Wiener increments such that $\mathrm{d}W_{n,i}(z)\mathrm{d}W_{n,j}(z) = \delta_{i,j}\mathrm{d}z/3$, with $i,j \in \{1,2,3\}$, where by $\delta_{i,j}$ we denote the Kronecker delta [30,31,38]. Using the rules of stochastic calculus [30], one can find the following equation for the increment of $\mathbf{U}_n(z,0)$,

$$\mathrm{d}\mathbf{U}_n = i\sqrt{D_n}\,\frac{\mathrm{d}\vec{W}_n\cdot\vec{\sigma}}{2}\mathbf{U}_n - \frac{D_n}{8}\mathbf{U}_n\mathrm{d}z, \tag{39}$$

where the second term at the right-hand side of the equality is known as the Ito correction. By performing the ensemble average of the above, and dividing by $\mathrm{d}z$ we obtain

$$\frac{\mathrm{d}\langle\mathbf{U}_n\rangle}{\mathrm{d}z} = -\frac{D_n}{8}\langle\mathbf{U}_n\rangle = -\frac{\pi^2 L_{C,n}}{L_{B,n}^2}\langle\mathbf{U}_n\rangle, \tag{40}$$

where we used the property of $\mathrm{d}\vec{W}_n(z)$ being uncorrelated with $\mathbf{U}_n(z,0)$. Solving the above yields Eq. (20).

Derivation of $\langle \mathbf{U}_n(z,0)\rangle$ *within the FMM*

Within the FMM [32] the birefringence vector lies in the equatorial plane of Stokes space, its length is constant and equals $2\pi/L_B$, and its direction $\theta_n(z)$ evolves along the fiber as a Wiener process [30],

$$\vec{\beta}_n = \frac{2\pi}{L_{B,n}}\left\{\cos[\theta_n(z)]\hat{s}_1 + \sin[\theta_n(z)]\hat{s}_2\right\}, \tag{41}$$

$$\mathrm{d}\theta_n = \sqrt{\frac{2}{L_{C,n}}}\mathrm{d}W_n \tag{42}$$

with $\mathrm{d}W^2 = \mathrm{d}z$, where by $\hat{s}_1$, $\hat{s}_2$, and $\hat{s}_3$ we denote the vectors of an orthonormal basis for Stokes space. Using the rules of stochastic calculus [30], one can find the increment of $\vec{\beta}_n$,

$$\mathrm{d}\vec{\beta}_n = (\hat{s}_3\times\vec{\beta})\mathrm{d}\theta_n - \frac{1}{L_C}\vec{\beta}_n\mathrm{d}z, \tag{43}$$

which can be used to prove the autocorrelation function Eq. (17). We now proceed to evaluate $\langle\mathbf{U}_n(z)\rangle$. The evolution equation obtained from Eq. (7),

$$\frac{\mathrm{d}\langle\mathbf{U}_n\rangle}{\mathrm{d}z} = \frac{i}{2}\langle(\vec{\beta}_n\cdot\vec{\sigma})\mathbf{U}_n\rangle, \tag{44}$$

implies evaluating the average $\langle(\vec{\beta}_n\cdot\vec{\sigma})\mathbf{U}_n\rangle$. The increment of the latter is $\mathrm{d}[(\vec{\beta}_n\cdot\vec{\sigma})\mathbf{U}_n] = (\mathrm{d}\vec{\beta}_n\cdot\vec{\sigma})\mathbf{U}_n + (\vec{\beta}_n\cdot\vec{\sigma})\mathrm{d}\mathbf{U}_n$, and the result of performing the ensemble average and dividing by $\mathrm{d}z$ is

$$\frac{\mathrm{d}\langle(\vec{\beta}_n\cdot\vec{\sigma})\mathbf{U}_n\rangle}{\mathrm{d}z} = -\frac{1}{L_{C,n}}\langle(\vec{\beta}_n\cdot\vec{\sigma})\mathbf{U}_n\rangle + \frac{i}{2}b_n^2\langle\mathbf{U}_n\rangle, \tag{45}$$

Optics EXPRESS

where we used the property of $\mathrm{d}W(z)$ being uncorrelated with all other quantities evaluated at z, as well as the known relation [18]

$$(\vec{\beta}_n \cdot \vec{\sigma})^2 = |\vec{\beta}_n|^2 \, \mathbf{I}. \tag{46}$$

We now perform a Laplace transform of Eqs. (44) and (45) with the initial conditions $\mathbf{U}_n(0) = \mathbf{I}$ and $\langle \vec{\beta}_n(0) \cdot \vec{\sigma}) \mathbf{U}_n(0) \rangle = 0$, which yields

$$s\mathcal{L}\left[\langle \mathbf{U}_n \rangle\right] - \mathbf{I} = -\frac{|\vec{\beta}_n|^2}{4(s + L_{C,n}^{-1})} \mathcal{L}\left[\langle \mathbf{U}_n \rangle\right], \tag{47}$$

where by $\mathcal{L}\left[f(z)\right] = \int_0^\infty \mathrm{d}z f(z) \exp(-sz)$ we denote the Laplace transform of f, with the result

$$\mathcal{L}\left[\langle \mathbf{U}_n \rangle\right] = \frac{s + L_{C,n}^{-1}}{s^2 + L_{C,n}^{-1} s + |\vec{\beta}_n|^2/4} \mathbf{I} = \mathcal{L}\left[R_n\right] \mathbf{I}. \tag{48}$$

For $L_{B,n} \neq 2\pi L_{C,n}$ the polynomial at the denominator has two distinct poles and one can readily obtain

$$\mathcal{L}\left[R_n\right] = \left(\frac{Z_n^{(1)}}{s - Y_n^{(1)}} + \frac{Z_n^{(2)}}{s - Y_n^{(2)}} \right) \tag{49}$$

where $Z_n^{(1,2)}$ and $Y_n^{(1,2)}$ are the ones given in Eqs. (33) and (32) if we use that in the FMM we have $|\vec{\beta}_n| = 2\pi / L_{B,n}$. If instead one uses in (48) $L_{B,n} = 2\pi L_{C,n}$, then $\mathcal{L}\left[R_n\right]$ can be decomposed as

$$\mathcal{L}\left[R_n\right] = \frac{1}{s + L_{C,n}^{-1}} + \frac{1}{2L_{C,n}} \frac{1}{\left(s + L_{C,n}^{-1}\right)^2}, \tag{50}$$

and its inverse Laplace transform is

$$R_n(z) = \left(1 + \frac{|z|}{2L_{C,n}}\right) e^{-\frac{|z|}{2L_{C,n}}}. \tag{51}$$

Finally, it is worth noting that the limit of $R_n(z)$ for large correlation lengths $L_{C,n} \gg L_{B,n}$ reads

$$R_n(z) = e^{-\frac{|z|}{2L_{C,n}}} \cos\left(\frac{\pi}{L_{B,n}} z\right). \tag{52}$$

The above equation extends to any z the results obtained for $|z| \ll L_{C,n}$.

Non-uniform coupling coefficient κ_{nm}

Let us decompose the coupling coefficient $\kappa_{nm}(z)$ as

$$\kappa_{nm}(z) = \kappa_{nm} + \Delta\kappa_{nm}(z'), \tag{53}$$

where κ_{nm} is a constant term and $\Delta\kappa_{nm}(z)$ are zero-average fluctuations, which may originate, for instance, by core-to-core fluctuations [20]. The use of this decomposition into Eq. (11) gives the expression of the crosstalk power as $P'_{nm} = P_{nm} + \Delta P_{nm}$, where P_{nm} is given by Eq. (11) with $\kappa_{nm}(z')\kappa_{nm}(z'')$ replaced by κ_{nm}^2 and

$$\Delta P_{nm} = \int_0^z \mathrm{d}z' \int_0^z \mathrm{d}z'' e^{i\Delta\beta_{nm}(z'-z'')} R_\kappa(z'-z'') R_{ff}(z'-z'') \langle \vec{e}_m^\dagger(z') \mathbf{U}_n(z', z'') \vec{e}_m(z'') \rangle, \tag{54}$$

where $R_\kappa(z'-z'') = \langle \Delta\kappa_{nm}^*(z') \Delta\kappa_{nm}(z'') \rangle$. We averaged the fluctuations of the coupling coefficient independently of the other terms because they are random and independent of scalar and intra-core

Optics EXPRESS

polarization coupling. The fluctuations of the coupling coefficient occur on top of a larger average value, and therefore their effect is to add the small term ΔP_{nm} to the large value P_{nm}. This is at variance with random polarization coupling and twist-bending, which act as zero-average dephasing mechanisms and are therefore multiplicative.

Assuming a two-sided exponential expression for R_κ, namely $R_\kappa(z) = \exp(-|z|/\ell_\kappa)$, and replacing R_{ff} with $R_{ff}R_\kappa$, yields

$$\Delta P_{nm} = \frac{\langle|\Delta\kappa_{nm}|^2\rangle}{\kappa_{nm}^2} P_{nm}, \tag{55}$$

where P_{nm} is the result obtained for constant $\kappa_{nm}(z) = \kappa_{nm}$ and with ℓ_c replaced by $(\ell_c^{-1} + \ell_\kappa^{-1})^{-1}$. The theory developed in the main text can be then straightforwardly used in the evaluation of ΔP_{nm}. The simplest cases are those in which $\ell_\kappa \gg \ell_c$ and all those in which P_{nm} is dominated by polarization effects. In these cases, the effect of the fluctuations is simply to increase of the coupling coefficient from κ_{nm}^2 to $\kappa_{nm}^2 + |\Delta\kappa_{nm}|^2$.

Equation (55) shows that if the variances of the coupling coefficients are limited to a few percentage points, the term ΔP_{nm} adds to P_{nm} a contribution of the same order, thus justifying the choice of neglecting the fluctuations of the coupling coefficient done in this paper.

Numerical simulations

All numerical simulations were carried out using the RMM with linear birefringence only [32]. Therefore, the first and second component of the birefringence vector where produced as independent Ornstein-Uhlenbeck processes [30] with a correlation function given by Eq. (17), while the third component was set to zero. In the numerical procedure we modeled the fiber as a concatenation of wave-plates of length Δz, so that propagation through the k-th section was described by the equation

$$\begin{bmatrix} \vec{E}_1(z_k) \\ \vec{E}_2(z_k) \\ \vec{E}_3(z_k) \\ \vec{E}_4(z_k) \end{bmatrix} = \exp\left[i \begin{pmatrix} \frac{\vec{\beta}_{1,k}\cdot\vec{\sigma}}{2} & \kappa\mathbf{I} & \mathbf{0} & \kappa\mathbf{I} \\ \kappa\mathbf{I} & \frac{\vec{\beta}_{2,k}\cdot\vec{\sigma}}{2} & \kappa\mathbf{I} & 0 \\ 0 & \kappa\mathbf{I} & \frac{\vec{\beta}_{3,k}\cdot\vec{\sigma}}{2} & \kappa\mathbf{I} \\ \kappa\mathbf{I} & 0 & \kappa\mathbf{I} & \frac{\vec{\beta}_{4,k}\cdot\vec{\sigma}}{2} \end{pmatrix} \Delta z \right] \begin{bmatrix} \vec{E}_1(z_{k-1}) \\ \vec{E}_2(z_{k-1}) \\ \vec{E}_3(z_{k-1}) \\ \vec{E}_4(z_{k-1}) \end{bmatrix}, \tag{56}$$

where $\vec{\beta}_{n,k}$ is the birefringence vector of core n. The step size was set to be significantly smaller than the birefringence correlation length, so that the birefringence vector could be safely assumed to be constant within each step. In particular we sampled the underlying Ornstein-Uhlenbeck processes with a spacing of $L_C/20$. The Ornstein-Uhlenbeck processes were generated with a resolution ten times greater by numerically filtering spatially white Gaussian noise,

$$\beta(z_k) = \sqrt{\frac{4\pi}{L_B L_C}} \int_{-\infty}^{z_k} e^{-\frac{z_k - z'}{L_C}} \mathrm{d}N(z'), \tag{57}$$

with $\langle N(z')N(z'')\rangle = \delta(z' - z'')$, and where we dropped some of the subscripts for ease of notation. The crosstalk was then evaluated as the field intensity in core 4, $|\vec{E}_4(z_k)|^2$, when only core 1 was excited at the fiber input with a field of random polarization and unit intensity. The crosstalk coefficient shown in Fig. 1 was extracted by fitting the crosstalk-vs-z curve at sufficiently large propagation distance, where the crosstalk was seen to accumulate linearly with distance.

Funding

Ministero dell'Istruzione, dell'Università e della Ricerca (FIRST, PRIN 2017); Italian Government (INCIPICT).

Optics EXPRESS

Acknowledgments

Insightful discussions with Prof. Luca Palmieri are acknowledged.

Disclosures

The authors declare no conflicts of interest.

References

1. P. J. Winzer and D. T. Neilson, "From scaling disparities to integrated parallelism: A decathlon for a decade," J. Lightwave Technol. **35**(5), 1099–1115 (2017).
2. M.-J. Li and T. Hayashi, "Chapter 1 - advances in low-loss, large-area, and multicore fibers," in *Optical Fiber Telecommunications VII*, A. E. Willner, ed. (Academic Press, 2020), pp. 3–50.
3. J. M. Fini, B. Zhu, T. F. Taunay, and M. F. Yan, "Statistics of crosstalk in bent multicore fibers," Opt. Express **18**(14), 15122–15129 (2010).
4. K. Takenaga, Y. Arakawa, S. Tanigawa, N. Guan, S. Matsuo, K. Saitoh, and M. Koshiba, "An investigation on crosstalk in multi-core fibers by introducing random fluctuation along longitudinal direction," IEICE Trans. Commun. **E94-B**(2), 409–416 (2011).
5. T. Hayashi, T. Taru, O. Shimakawa, T. Sasaki, and E. Sasaoka, "Design and fabrication of ultra-low crosstalk and low-loss multi-core fiber," Opt. Express **19**(17), 16576–16592 (2011).
6. M. Koshiba, K. Saitoh, K. Takenaga, and S. Matsuo, "Multi-core fiber design and analysis: coupled-mode theory and coupled-power theory," Opt. Express **19**(26), B102–B111 (2011).
7. M. Koshiba, K. Saitoh, K. Takenaga, and S. Matsuo, "Analytical expression of average power-coupling coefficients for estimating intercore crosstalk in multicore fibers," IEEE Photonics J. **4**(5), 1987–1995 (2012).
8. T. Hayashi, T. Sasaki, E. Sasaoka, K. Saitoh, and M. Koshiba, "Physical interpretation of intercore crosstalk in multicore fiber: effects of macrobend, structure fluctuation, and microbend," Opt. Express **21**(5), 5401–5412 (2013).
9. T. Hayashi, H. Chen, N. K. Fontaine, T. Nagashima, R. Ryf, R. Essiambre, and T. Taru, "Effects of core count/layout and twisting condition on spatial mode dispersion in coupled multi-core fibers," in *ECOC 2016; 42nd European Conference on Optical Communication*, (2016), pp. 1–3.
10. T. Fujisawa, Y. Amma, Y. Sasaki, S. Matsuo, K. Aikawa, K. Saitoh, and M. Koshiba, "Crosstalk analysis of heterogeneous multicore fibers using coupled-mode theory," IEEE Photonics J. **9**(5), 1–8 (2017).
11. T. Hayashi, T. Nagashima, T. Muramoto, F. Sato, and T. Nakanishi, "Spatial mode dispersion suppressed randomly-coupled multi-core fiber in straightened loose-tube cable," in *Optical Fiber Communication Conference Postdeadline Papers 2019*, (Optical Society of America, 2019), p. Th4A.2.
12. K. Nishimura, T. Sato, T. Fujisawa, Y. Amma, K. Takenaga, K. Aikawa, and K. Saitoh, "Cladding diameter dependence of inter-core crosstalk in heterogeneous multicore fibers," in *2019 24th OptoElectronics and Communications Conference (OECC) and 2019 International Conference on Photonics in Switching and Computing (PSC)*, (2019), pp. 1–3.
13. Y. Amma, Y. Sasaki, K. Takenaga, S. Matsuo, J. Tu, K. Saitoh, M. Koshiba, T. Morioka, and Y. Miyamoto, "High-density multicore fiber with heterogeneous core arrangement," in *2015 Optical Fiber Communications Conference and Exhibition (OFC)*, (2015), pp. 1–3.
14. A. V. T. Cartaxo and T. M. F. Alves, "Discrete changes model of inter-core crosstalk of real homogeneous multi-core fibers," J. Lightwave Technol. **35**(12), 2398–2408 (2017).
15. R. O. J. Soeiro, T. M. F. Alves, and A. V. T. Cartaxo, "Dual polarization discrete changes model of inter-core crosstalk in multi-core fibers," IEEE Photonics Technol. Lett. **29**(16), 1395–1398 (2017).
16. A. Macho, C. García-Meca, F. J. Fraile-Peláez, M. Morant, and R. Llorente, "Birefringence effects in multi-core fiber: coupled local-mode theory," Opt. Express **24**(19), 21415–21434 (2016).
17. A. Galtarossa, L. Palmieri, M. Schiano, and T. Tambosso, "Measurement of birefringence correlation length in long, single-mode fibers," Opt. Lett. **26**(13), 962–964 (2001).
18. J. P. Gordon and H. Kogelnik, "PMD fundamentals: Polarization mode dispersion in optical fibers," Proc. Natl. Acad. Sci. **97**(9), 4541–4550 (2000).
19. A. W. Snyder, "Coupled-mode theory for optical fibers," J. Opt. Soc. Am. **62**(11), 1267–1277 (1972).
20. C. Antonelli, A. Mecozzi, and M. Shtaif, "The delay spread in fibers for SDM transmission: dependence on fiber parameters and perturbations," Opt. Express **23**(3), 2196–2202 (2015).
21. C. Antonelli, A. Mecozzi, M. Shtaif, and P. J. Winzer, "Stokes-space analysis of modal dispersion in fibers with multiple mode transmission," Opt. Express **20**(11), 11718–11733 (2012).
22. G. Rademacher, R. S. Luís, B. J. Puttnam, Y. Awaji, and N. Wada, "Crosstalk-induced system outage in intensity-modulated direct-detection multi-core fiber transmission," J. Lightwave Technol. **38**(2), 291–296 (2020).
23. A. W. Snyder and A. Ankiewicz, "Optical fiber couplers-optimum solution for unequal cores," J. Lightwave Technol. **6**(3), 463–474 (1988).
24. W.-P. Huang, "Coupled-mode theory for optical waveguides: an overview," J. Opt. Soc. Am. A **11**(3), 963–983 (1994).

Optics EXPRESS

25. We note that the same conclusion holds when accounting for the fluctuations of the coupling coefficient κ_{nm}, as their contribution is of the same form as in Eq. (13), as pointed out in the Appendix.
26. In general, the presence of the function $R_n(z)$ and $R_m(z)$ may also result into an increase of the average crosstalk, depending on whether their product and/or $R_{ff}(z)$ are complex-valued.
27. P. K. A. Wai and C. R. Menyuk, "Polarization decorrelation in optical fibers with randomly varying birefringence," Opt. Lett. **19**(19), 1517–1519 (1994).
28. A. Galtarossa, L. Palmieri, M. Schiano, and T. Tambosso, "PMD in single-mode fibers: measurements of local birefringence correlation length," in *OFC 2001. Optical Fiber Communication Conference and Exhibit. Technical Digest Postconference Edition (IEEE Cat. 01CH37171)*, vol. 4 (2001), pp. ThA2–ThA2.
29. A. Galtarossa and L. Palmieri, "Measure of twist-induced circular birefringence in long single-mode fibers: theory and experiments," J. Lightwave Technol. **20**(7), 1149–1159 (2002).
30. C. Gardiner, *Handbook of stochastic methods for physics, chemistry, and the natural sciences*, Springer series in synergetics (Springer-Verlag, 1985).
31. J. P. Gordon, *Statistical properties of polarization mode dispersion* (Springer New York, New York, NY, 200552–59
32. A. Galtarossa, L. Palmieri, A. Pizzinat, B. S. Marks, and C. R. Menyuk, "An analytical formula for the mean differential group delay of randomly birefringent spun fibers," J. Lightwave Technol. **21**(7), 1635–1643 (2003).
33. A. Pizzinat, B. S. Marks, L. Palmieri, C. R. Menyuk, and A. Galtarossa, "Influence of the model for random birefringence on the differential group delay of periodically spun fibers," IEEE Photonics Technol. Lett. **15**(6), 819–821 (2003).
34. The third case $L_{B,n} = 2\pi L_{C,n}$ is of no practical relevance and is covered in the Appendix.
35. A. Galtarossa, L. Palmieri, M. Schiano, and T. Tambosso, "Measurements of beat length and perturbation length in long single-mode fibers," Opt. Lett. **25**(6), 384–386 (2000).
36. C. Antonelli, A. Mecozzi, M. Shtaif, and P. J. Winzer, "Random coupling between groups of degenerate fiber modes in mode multiplexed transmission," Opt. Express **21**(8), 9484–9490 (2013).
37. T. M. F. Alves, R. O. J. Soeiro, and A. V. T. Cartaxo, "Probability distribution of intercore crosstalk in weakly coupled mcfs with multiple interferers," IEEE Photonics Technol. Lett. **31**(8), 651–654 (2019).
38. M. Shtaif and A. Mecozzi, "Study of the frequency autocorrelation of the differential group delay in fibers with polarization mode dispersion," Opt. Lett. **25**(10), 707–709 (2000).